Characterisation of metal organic frameworks for adsorption cooling

Ahmed Rezk, Raya Al-Dadah *, Saad Mahmoud, Ahmed Elsayed

Department of Mechanical Engineering, University of Birmingham, Birmingham, Edgbaston, B15 2TT, United Kingdom

A B S T R A C T

Silica gel/water adsorption cooling systems suffer from size, performance and cost limitations. Therefore, there is a need for new adsorbent materials that outperform silica gel. Metal organic frameworks (MOFs) are new micro-porous materials that have extraordinary porosity and uniform structure. Due to the lack of published data that characterise MOF/water adsorption, this paper experimentally investigates the adsorption characteristics of HKUST-1 (Cu-BTC (copper benzene-1,3,5-tricarboxylate), $C_{18}H_6Cu_3O_{12}$) and MIL-100 (Fe-BTC (Iron 1,3,5-benzenetricarboxylate), $C_9H_3FeO_6$) MOFs compared to silica gel RD-2060. The adsorption characteristics of Silica gel RD-2060, HKUST-1 and MIL-100 were determined using an advanced gravimetric dynamic vapour sorption analyser (DVS). Results showed that HKUST-1 performed better than silica gel RD-2060 with an increase of water uptake of 93.2%, which could lead to a considerable increase in refrigerant flow rate, cooling capacity and/or reducing the size of the adsorption system. However, MIL-100 MOF showed reduced water uptake comparable to silica gel RD-2060 for water chilling applications with evaporation at 5 ^{0}C. These results highlight the potential of using MOF materials to improve the efficiency of water adsorption cooling systems.

1. Introduction

Silica gel has been investigated as water adsorbent for a number of cooling applications [1–3] including combined power, heating and cooling (known as Trigeneration) [4,5], automotive air conditioning [6] and solar powered cooling systems [7,8]. However, one of the silica gel problems as adsorbent is that most of water adsorption occurs at high partial pressure. This means that the amount of water vapour adsorbed/desorbed in a cycle of normal operating conditions is only a small part of the total adsorption capacity of the silica gel [9,10] resulting in silica gel/water adsorption cooling systems having large footprint and high capital cost [11,12]. Therefore there is a need for new adsorbent material that can adsorb water at lower partial pressures than that of silica gel.

Metal organic frameworks (MOFs) are new micro-porous materials with exceptionally high porosity, uniform structure and large surface area (up to 5500 m^2/g) which have attracted a considerable scientific interest recently [13,14]. These were initially investigated for gas storage applications such as hydrogen and methane [15,16]. MOFs structures consists of two main components: the organic linkers considered as organic secondary building unit, act as struts that bridge metal centres known as inorganic primary building units and act as joints in the resulting MOF architecture. These components are connected to each other by coordination bonds to form a network with defined topology [17,18]. MOFs are classified into two kinds: the zinc-based and other metals-based. Metals that have been studied for MOFs synthesis are aluminium, copper, chromium, manganese, iron, zirconium and scandium [13,14]. Research by Henninger et al. [10] indicated the potential of applying MOFs materials for water adsorption cooling systems. However, limited work regarding their water adsorption characterisation and cyclic performance was reported.

This paper experimentally investigates the water adsorption characteristics of two types of MOFs; namely HKUST-1 (copper based) and MIL-100 (iron based), in terms of adsorption isotherms, isosteric heat of adsorption and adsorption kinetics for temperatures up to 52 °C. Cyclic analysis up to 85 °C was investigated using developed correlations based on the experimental data. These MOFs are commercially named Basolite C300® and Basolite F300®, manufactured by BASF, USA and marketed by Sigma Aldrich UK. HKUST-1 is selected because it is one of the first robust metal organic polymers made with a microporous structure that is reminiscent of the topology of zeolite framework [19]. MIL-100 is selected due to its stability during hot water treatment [17]. Also the performance of silica gel RD-2060 was investigated as a reference material. Fig. 1 presents SEM images of HKUST-1, MIL-100 and silica gel RD-2060 and Table 1 presents the chemical formula, granular size, BET surface area and bulk density for these materials.

2. Experimental work

The adsorption characteristics that affect the chiller performance are adsorption isotherms, isosteric heat of adsorption and

* Corresponding author.
E-mail address: r.k.al-dadah@bham.ac.uk (R. Al-Dadah).

Nomenclature

Symbol			
A_o	coefficient in Eq. (2) (kg/kg)	R_p	particle radius (m)
A_1	coefficient in Eq. (2) (kg/kg K)	T	temperature (K)
A_2	coefficient in Eq. (2) (kg/kg K^3)	t	time (s)
A_3	coefficient in Eq. (2) (kg/kg K^3)	W	uptake value (kg_{water}/kg_{silica})
B_o	coefficient in Eq. (3) (K)	$w*$	equilibrium uptake (kg_{water}/kg_{silica})
B_1	coefficient in Eq. (3) (K^{-1})	Δ	difference
B_2	coefficient in Eq. (3) (K^{-2})		
B_3	coefficient in Eq. (3) (K^{-3})	Subscripts	
D_{so}	pre-exponential constant (m^2/s)	ads	adsorbent
ΔH_a	isosteric heat of adsorption (J/kg)	ref	refrigerant
E_a	activation energy (J/mol)	s	silica gel RD-2060
$K_s a_v$	overall mass transfer coefficient (kW/m K)	sat	saturation
P	pressure (kPa)	i	time index
R	Universal gas constant (J/mol K)	w	water

adsorption kinetics. There are two methods for measuring adsorption characteristics namely; volumetric method and gravimetric method [20,21]. In this investigation a dynamic vapour sorption (DVS) gravimetric analyser has been used to study the water adsorption characteristics (adsorption isotherms, kinetics and isosters) of the selected adsorbents, Fig. 2. In this DVS analyser, the adsorbent mass is measured directly using sensitive recording microbalance (Cahn D200) which has high long-term stability as it adsorbs controlled concentrations of water or organic vapours. Dry Nitrogen is used to purge the balance head and reaction chamber prior to sample loading. The purge flow is automatically controlled to prevent vapour condensation in the balance head and hence accurate uptake measurement is guaranteed. The microbalance is housed in a controlled temperature chamber to avoid vapour condensation in connections. Mass flow controller is used to control the vapour pressure with a mixture of dry and saturated vapour gas. The test conditions were measured using optical vapour pressure sensor and RTD temperature probe very close to sample pan. The DVS analyser is controlled by a PC microcomputer, which is interfaced with the microbalance. The accuracy of the DVS

Table 1
Physical properties of tested materials.

Property	HKUST-1	MIL-100	Silica gel RD-2060
Chemical Formula	$C_{18}H_6Cu_3O_{12}$	$C_9H_3FeO_6$	SiO_2
Granules size	16 μm	5 μm	0.18–1 mm
BET surface area	1500–2100 m^2/g	1300–1600 m^2/g	840 m^2/g
Bulk density	0.35 g/cm^3	0.16–0.35 g/cm^3	1 g/cm^3

analyser microbalance Cahn is verified by using 100 mg standard calibration mass, where the expected mass accuracy of the tested sample is ±0.05 mg.

Samples of 10 mg (±0.05 mg) each has been placed in the reaction chamber. All samples were dried until the condition of no change of mass is reached (Fig. 3 shows such drying process at 36 °C), then adsorption/desorption processes at various partial pressures were carried out. The sample mass is recorded every 4 s at different vapour pressure value to determine the adsorption kinetics. The sample isotherms are measured at each value of
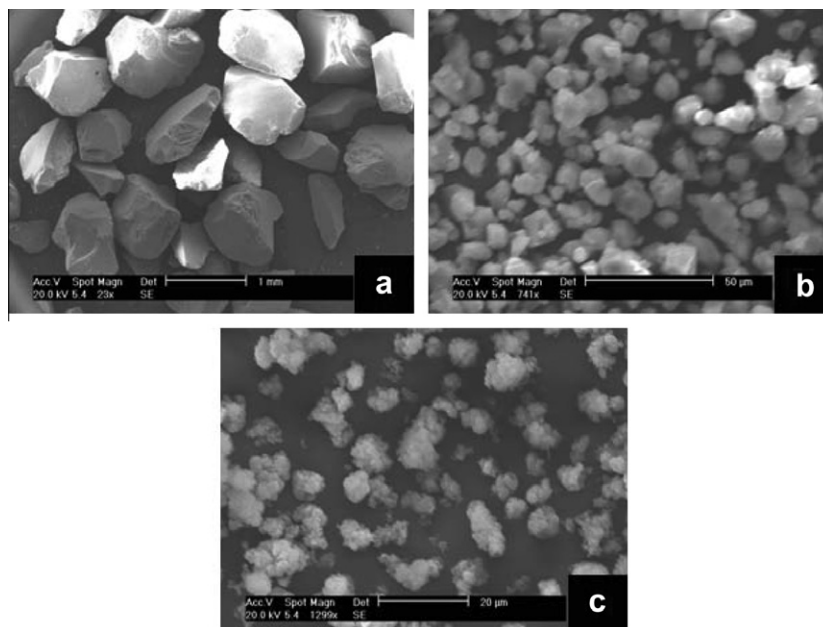
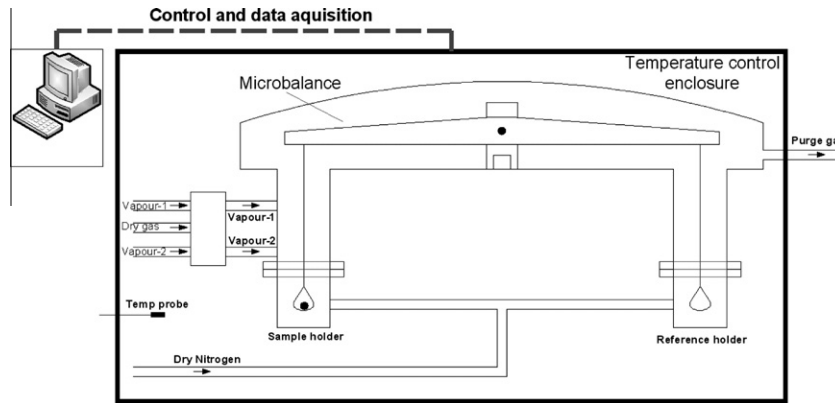**Fig. 1.** SEM images for (a) Silica gel RD-2060 (b) HKUST-1 (c) MIL-100.
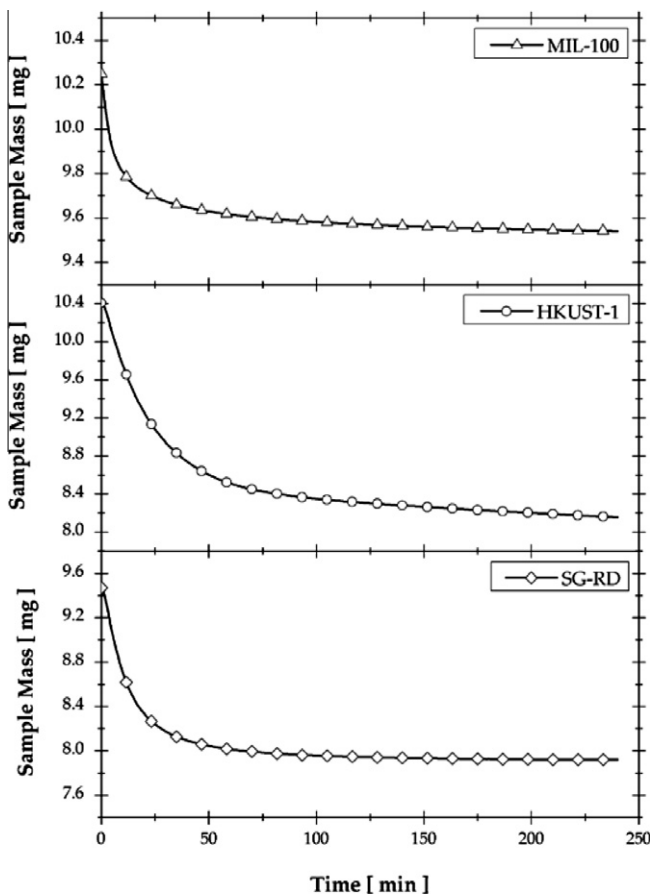
Fig. 2. Pictorial view of the used DVS instrument.

Fig. 3. Drying curves for different adsorbents at 36 °C.

Fig. 4. Temporal water vapour uptake at various vapour pressures for silica gel RD-2060 at $T = 36$ °C.

with linear driving force model (LDF) [23–29] described by Eq. (1) and (2). In order to validate the measurement technique used, silica gel RD-2060 was tested and the results were compared to the Linear Driving Force model. Fig. 4 presents the measured water vapour uptake variation with time for silica gel RD-2060 using different vapour pressures at 36 ° and Fig. 5 compares the measured values to those predicted by the LDF model with maximum deviation of ±20%.

$$w = w^* - \exp[-k_s a_v \cdot t + \ln(w^* - w_t)] \tag{1}$$

Fig. 5. Comparison between the measured water vapour uptake of silica gel RD-2060 and those predicted by the LDF model.

vapour pressure at the point of no change in adsorbent mass by measuring the adsorbent uptake. For each adsorbent, this procedure (drying, adsorption and desorption) was conducted at temperatures ranging from 20℃ to 52℃ at a step of 8 degrees and vapour pressure ranging from 200 Pa to 10000 Pa.

In physical adsorption phenomena the intraparticle mass transfer resistance dominates interparticle resistance [22]. The key parameter of intraparticle mass transfer is the diffusion time constant which is directly proportional to the surface diffusion, but inversely proportional to the adsorbent granules size. The rate of intraparticle mass transfer for different adsorbent/adsorbate pairs is normally measured using the gravimetric analyser and modelled
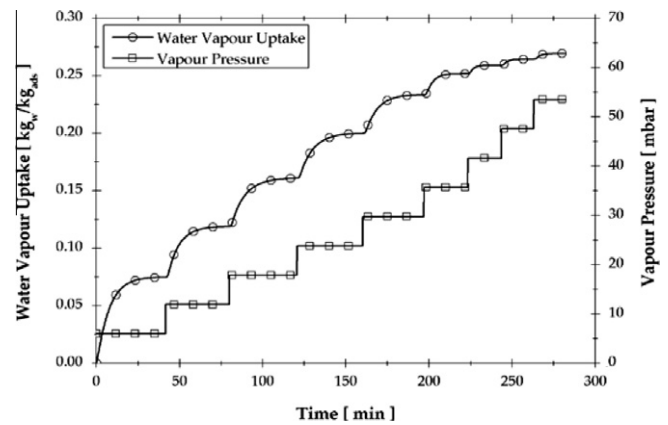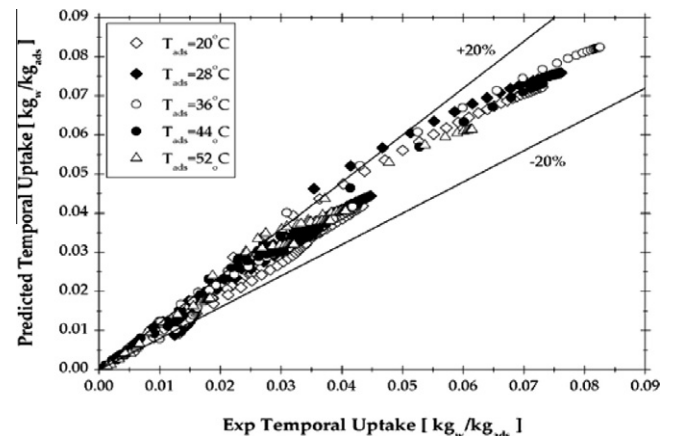
Table 2
Empirical constants for LDF model.

Parameter	Value	Unit
Silica gel RD-2060		
$F.D_{so}$	3.81×10^{-3}	m^2/s
E_a	4.2×10^4	J/mol
R_p	0.16×10^{-3}	m
HKUST-1		
$F.D_{so}$	4.08×10^{-3}	m^2/s
E_a	1.99×10^4	J/mol
R_p	8×10^{-6}	m
MIL-100		
$F.D_{so}$	2.63×10^{-3}	m^2/s
E_a	2.70×10^4	J/mol
R_p	2.5×10^{-6}	m

$$k_s a_v = (F.D_{so}/R_p^2)exp(-E_a/RT) \qquad (2)$$

where R_p, D_{so}, E_a, R and $w*$ are particles radius, pre-exponential constant, activation energy, universal constant and equilibrium uptake respectively and their values were given in Table 2 [27].

3. MOFs performance characterisation

Samples of MOF materials of HKUST-1 and MIL-100 are tested using the DVS analyser in order to characterise their adsorption isotherms, cyclic and kinetic performance compared to those of the reference material silica gel RD-2060.
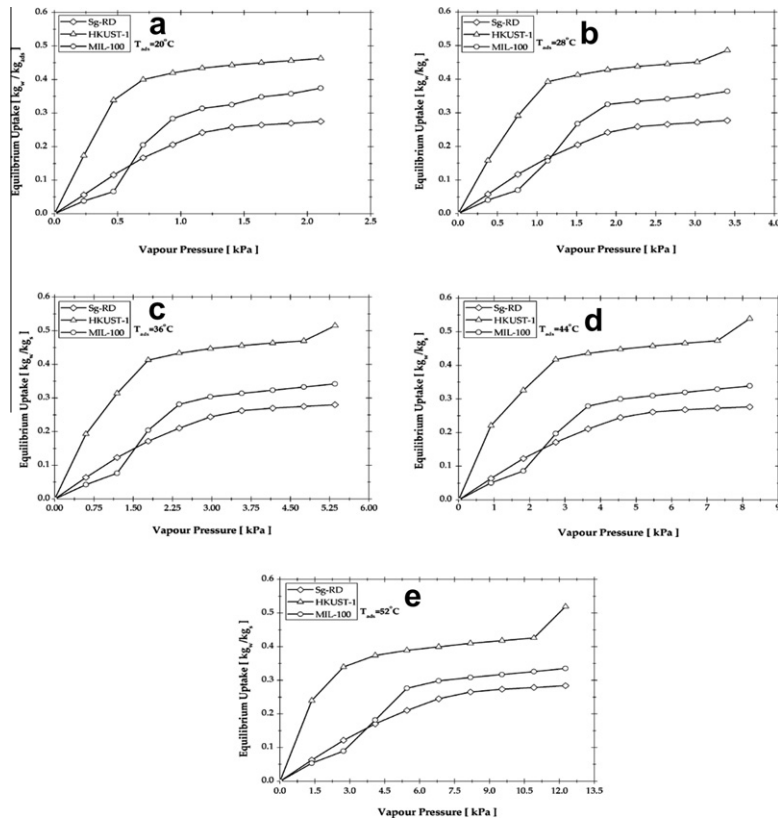
4. Adsorption Isotherms

The adsorption isotherm determines the amount of the adsorbed adsorbate over the dry mass of adsorbent as a function of its vapour pressure at constant temperature. Fig. 6 presents the adsorption isotherms for the tested HKUST-1 and MIL-100 compared to those of silica gel RD-2060 for the temperatures 20, 28, 36, 44 and 52 ^{0}C. This temperature range was dictated by the capability of the DVS used. Fig. 6 also shows that silica gel RD-2060, HKUST-1 and MIL-100 isotherms behave as type-I, type-II and type-V adsorbents respectively, based on Brunauer classification [30]. For all tested vapour pressures, HKUST-1 adsorbs more water vapour than the other adsorbents where the average maximum water vapour uptake value is 0.50 kg_w/kg_{ads} which is 78.6% higher than that of the tested silica gel RD-2060. Fig. 6 also shows that the MIL-100 has low water adsorption at low vapour pressure and higher value at higher vapour pressures. The average maximum equilibrium uptake value of MIL-100 is 0.35 kg_w/kg_{ads} which is 25% higher than that of silica gel RD-2060. Based on these results, the maximum equilibrium uptake is highest for HKUST-1 followed by MIL-100 and silica gel RD-2060.

Fig. 7 presents the ratio of the equilibrium water vapour uptake to its maximum value (percentage) versus the partial pressure for the three materials tested. It can be seen that HKUST-1 is more effective than silica gel RD-2060 in adsorbing water vapour closer to its maximum water uptake in particular at low partial pressure values. For example, HKUST-1 adsorbs 50% of its maximum capacity at partial pressure of 0.13 while silica gel RD-2060 adsorbs up 50% of its maximum capacity at partial pressure of 0.22. As for MIL-100, at partial pressure below 0.3, its performance is inferior to silica gel RD-2060 but it is slightly improved above the partial pressure of 0.3.

Fig. 8 shows the measured adsorption and desorption isotherms at 52 ^{0}C for all the materials tested. It is clear from this figure that both silica gel RD-2060 and MIL-100 have demonstrated little difference between the adsorption and desorption while HKUST-1 has shown clear hysteresis between adsorption and desorption.

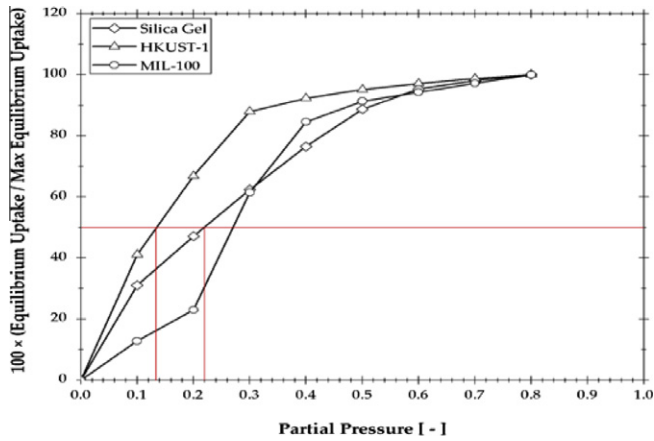**Fig. 6.** Adsorption isotherms comparison for different adsorbents.

Fig. 7. Ratio of water vapour equilibrium uptake to its maximum value versus partial pressure.

Isosteric analysis is one of the key characteristics that need to be studied. Ruthven [30] correlated the relation between vapour pressure (P_v), adsorbent temperature (T) and the isosteric heat of adsorption (ΔH_s) of adsorbent/refrigerant pairs as shown in Eq. (3). Table 3 presents the average calculated isosteric heat of adsorption based on the experimentally measured isotherms for water adsorption on silica gel RD-206, HKUST-1 and MIL100 compared to published values.

$$Ln(P_v) = \text{constant} - \Delta H_s/RT \tag{3}$$

where R is the Universal gas constant.

5. Adsorption kinetics

The adsorption kinetics should be considered during comparison between different adsorption pairs [25]. It determines the rate at which the adsorbent material adsorbs/desorbs the refrigerant. As outlined in the experimental procedure section, the sample mass is recorded every 4 seconds at different vapour pressure value to determine the adsorption kinetics. Fig. 9 shows the measured water vapour uptake variation with time for HKUST-1 and MIL-100 using different vapour pressures at 36 ^{0}C. Measurements shown in Fig. 9 were then used to develop the LDF model (Eqs. (1) and (2)) for HKUST-1 and MIL-100 and Table 2 gives the empirical values of F.D_{so} and E_a. Fig. 10 compares the measured water uptake values with those predicted by the developed LDF model with a maximum deviation of ±15%. Fig. 11 compares the measured water vapour uptake versus time for all materials tested at different temperatures for a vapour pressure of 0.5 mbar. It is clear that HKUST-1 shows the maximum adsorption rate (highest adsorption kinetics) followed by silica gel RD-2060 and MIL-100. The faster adsorption rate of HKUST-1/water pair implies shorter adsorption/desorption [31] cycle than that of silica gel RD-2060.

6. Adsorption cycle analysis

In order to carry out the cycle analysis of the three materials tested, the isotherms for the required operating temperature range need to be established. In this work, the isotherms at the upper temperature range 85 ℃ were predicted based on the measured isotherms up to 52 ℃ and using established adsorption models. There are a number of adsorption isotherm models including Dubinin–Astakhov (D–A), Sips, Toth, Freundlich, Modified Freundlich, Langmuir and Temkin and Hill-de-Boer [32–35]. For silica gel RD-2060,
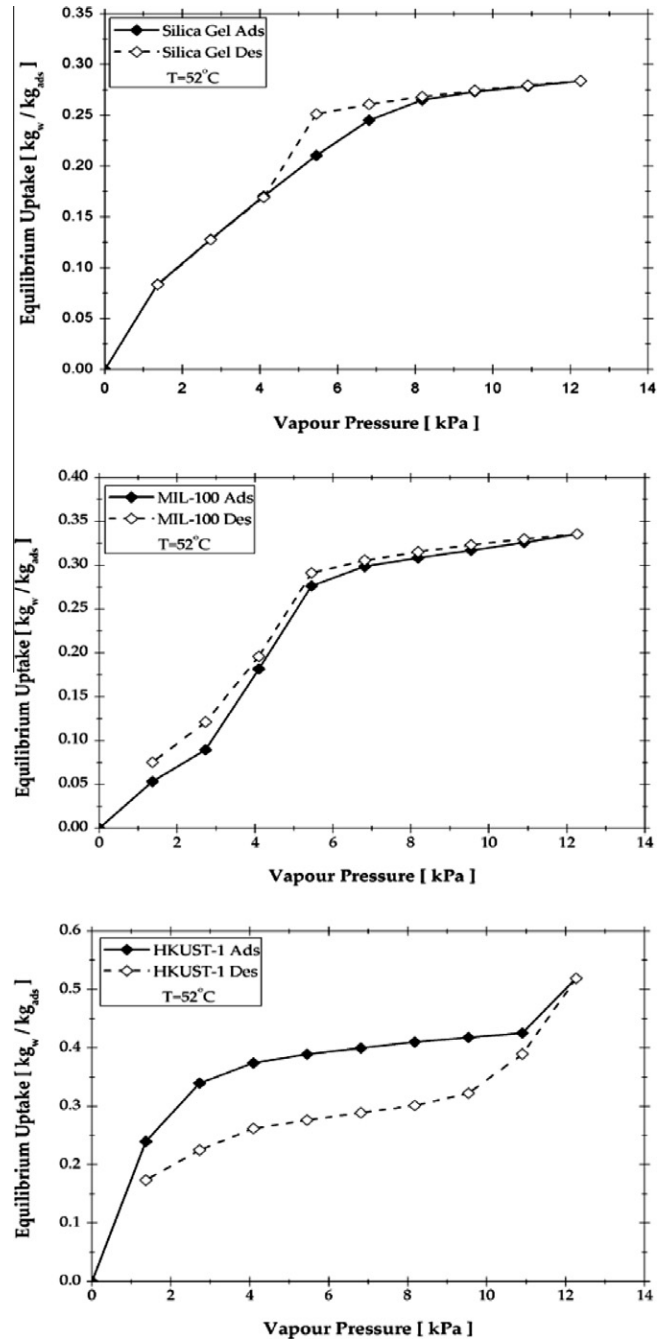

Fig. 8. Adsorption and desorption isotherms for silica gel RD-2060, MIL-100 and HKUST-1 at 52 °C.

Table 3
Isosteric heat of adsorption.

Author	ΔH_s (J/kg)	Deviation
Silica gel RD 2060		
Current work	2.43×10^6	
Wang [40] and Wang et al. [20]	2.51×10^6	3.2%
Wang et al., [21]	2.69×10^6	9.7%
Akahira et al., [41] and Uyun et al., [42]	2.80×10^6	13.2%
HKUST-1		
Current work	2.693×10^6	
Henninger et al., [10]	2.814×10^6	4.5%
MIL-100		
Current Work	2.632×10^6	
Kusgen et al., [17]	2.710×10^6	2.96%
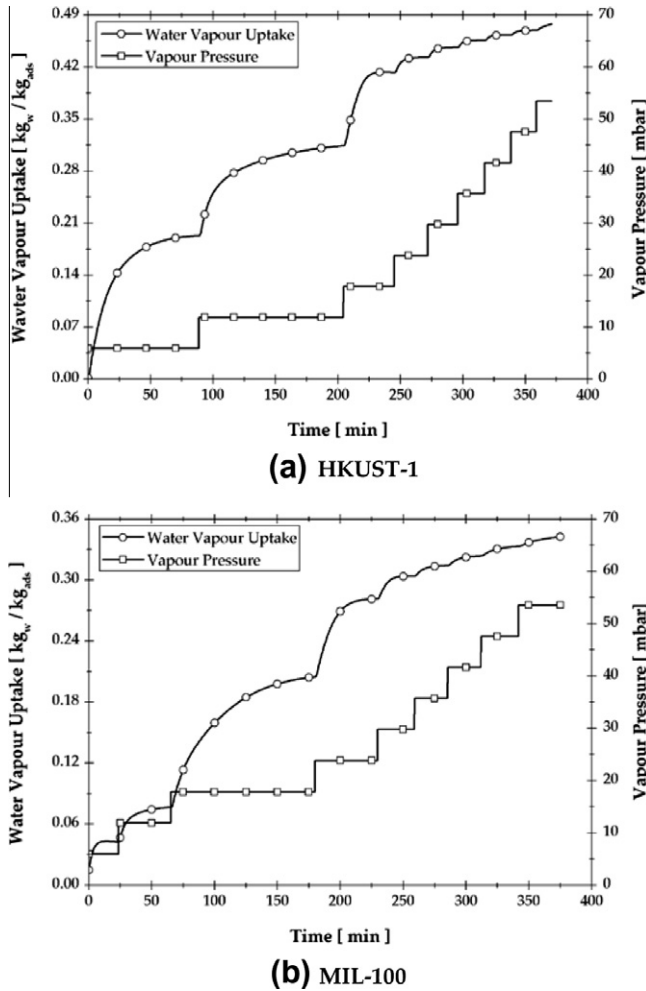
(a) HKUST-1

(b) MIL-100

Fig. 9. Temporal water vapour uptake at various vapour pressures at T = 36 °C.

(a) HKUST-1

(b) MIL-100

Fig. 10. Comparison between the measured water vapour uptake of HKUST-1 and MIL-100 and those predicted by the LDF model.

the Modified Freundlich model is used [36–37] while for HKUST-1 and MIL-100, Langmuir [38] and Sips models [39] are used.

Fig. 12 shows the adsorption isotherms for all tested materials up to 85 °C with isotherms measured at temperatures up to 52 °C and predicted for higher temperatures up to 85 °C. Fig. 10a shows the silica gel RD-2060 isotherms as predicted by the modified Freundlich model (Eq. (4)–(6) with constants given in Table 4) with the deviation between the experimental results and those predicted at temperatures up to 52 °C (solid lines) are found to be within ±16%. For HKUST-1, the measured isotherms were used to develop a correlation based on Langmuir model as given in equation 7 with W^∞ and b equal to 0.6576 and 4.548 respectively. Fig. 12b shows the predicted isotherms of HKUST-1 up to 85 °C with the deviation between the measured isotherms and those predicted by equation 4 up to 52 °C (solid lines) is ±15.5%. Similarly, the measured isotherms of MIL-100 were used to develop a correlation based on the Sips model as shown in equation 8 with W^∞, b and n equal to 0.3571, 3.508 and 3.2395 respectively. Fig. 12(c) shows the predicted isotherms up to 85 °C with the deviation between the measured isotherms and those predicted by equation 8 up to 52 °C (solid lines) is ±18.6%.

$$w^* = A(T_{ads})[P_{sat}(T_{ref})/P_{sat}(T_{ads})]^{B(T_{ads})} \tag{4}$$

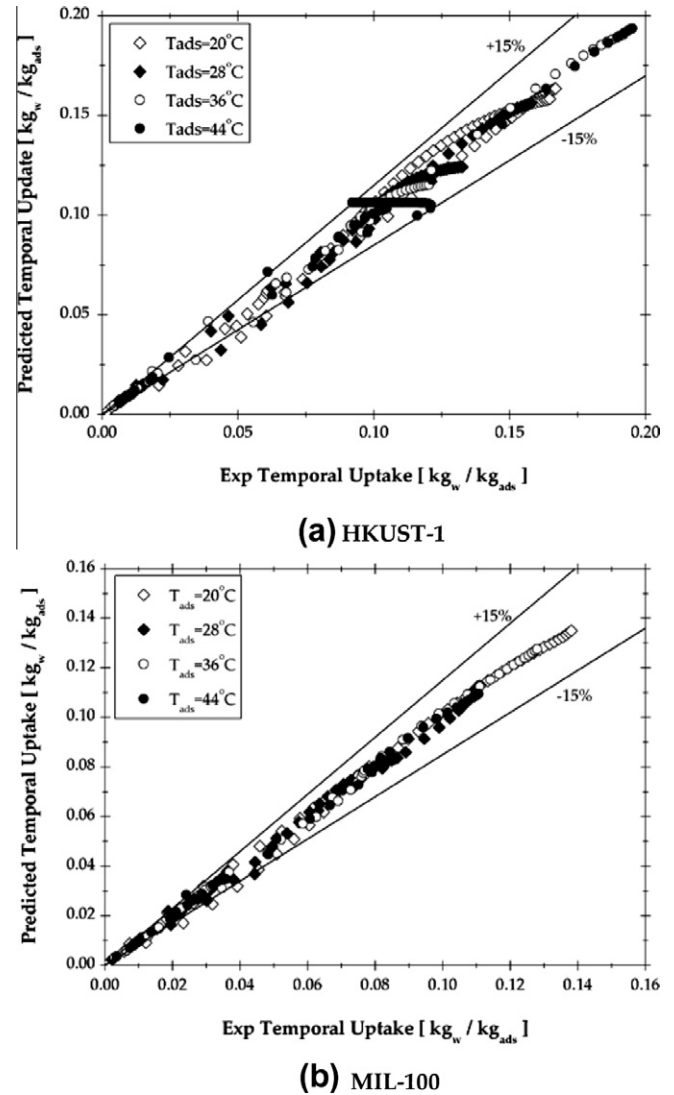$$A(T_{ads}) = A_0 + A_1 T_{ads} + A_2 T_{ads}^2 + A_3 T_{ads}^3 \tag{5}$$

$$B(T_{ads}) = B_0 + B_1 T_{ads} + B_2 T_{ads}^2 + B_3 T_{ads}^3 \tag{6}$$

$$w^* = W^\infty[b \cdot (P_{sat,T_{ref}}/P_{sat,T_{ads}})/(1 + b \cdot (P_{sat,T_{ref}}/P_{sat,T_{ads}}))] \tag{7}$$

$$w^* = W^\infty[(b \cdot P_{sat,T_{ref}}/P_{sat,T_{ads}})^n/(1 + (b \cdot P_{sat,T_{ref}}/P_{sat,T_{ads}})^n)] \tag{8}$$

The thermodynamic relation between pressures, adsorption temperatures and water vapour concentration is presented by the P-T-W (pressure-temperature-concentration) diagram where the concentration is defined as the mass of water vapour per unit mass of dry adsorbent. Fig. 13, presents the P-T-W diagram for HKUST-1, MIL-100 and silica gel RD-2060 with the ideal adsorption cooling cycle superimposed. For all the materials tested, the ideal adsorption cooling cycle consists of adsorption and condensation at 32 °C, desorption at 85 °C and evaporation at 5 °C typically used in chilled water systems. Fig. 13 also shows that the values of the water vapour concentration at the end of desorption/adsorption are 0.158/0.328 kg_w/kg_{ads}, 0.033/0.092 kg_w/kg_{ads} and 0.033/0.121 kg_w/kg_{ads} for HKUST-1, MIL-100 and silica gel RD-2060 respectively. It is clear that HKUST-1 has the highest values of water vapour concentration at the end of desorption/adsorption indicating higher rates of refrigerant circulation which leads to higher cooling capacities.
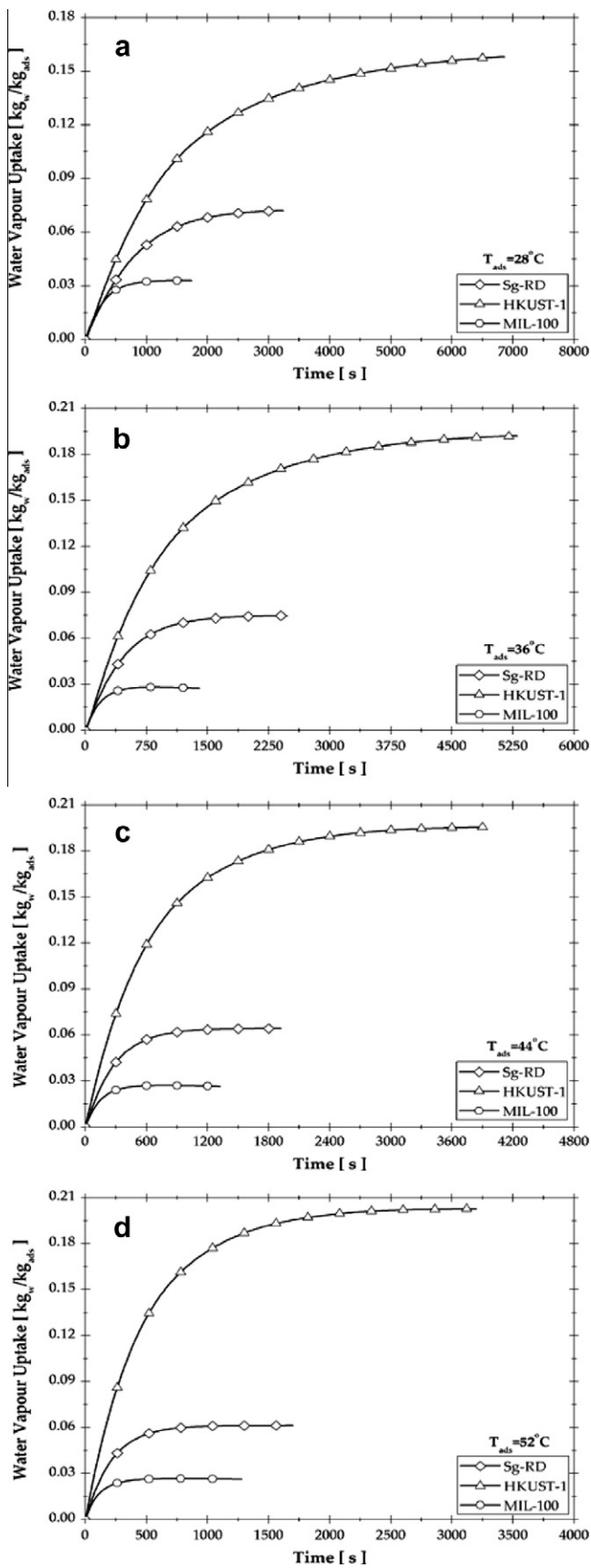
Fig. 11. Adsorption kinetics comparison for silica gel RD-2060, HKUST-1 and MIL-100 at vapour partial pressure of 0.1.
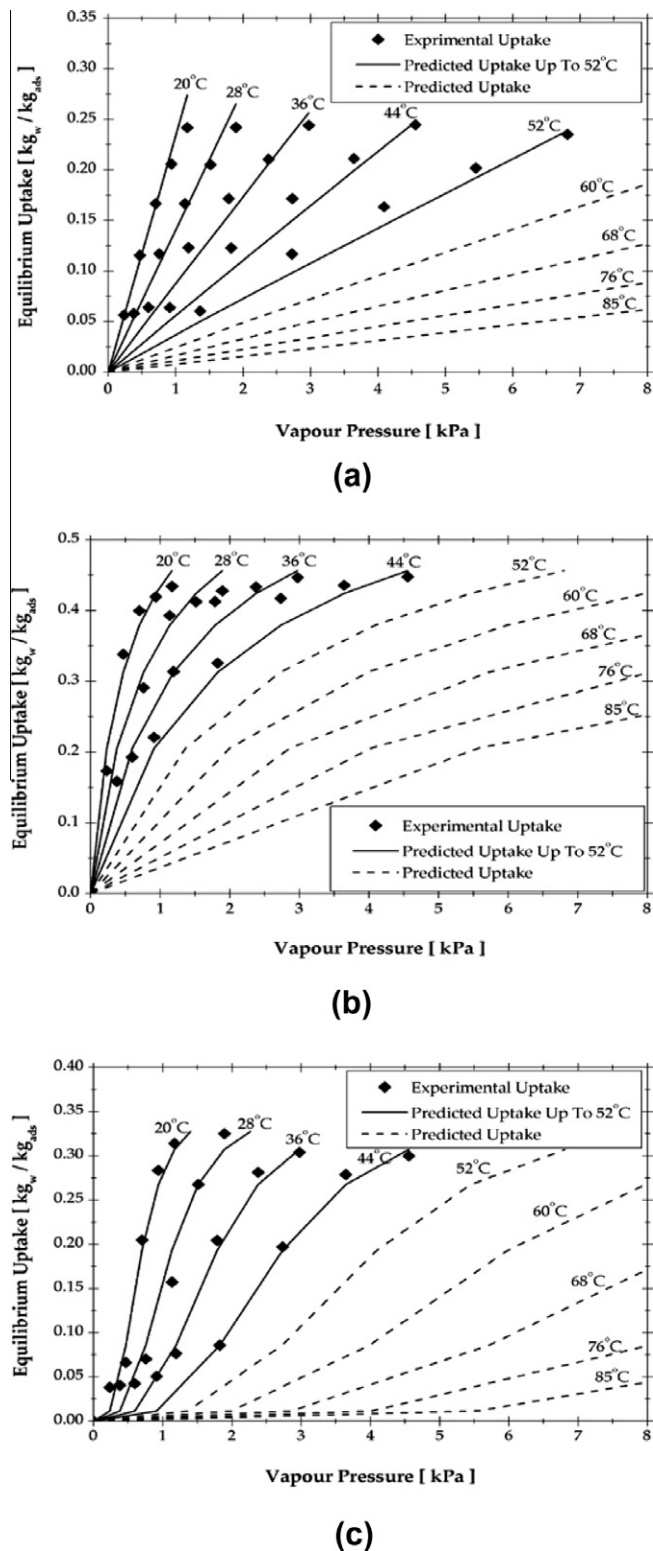

Fig. 12. Comparison between experimental and modified Freundlich isotherms.

Fig. 14 shows the ideal adsorption cooling cycle for HKUST-1 and MIL-100 (1-2-3-4-1) compared to that of silica gel RD-2060 (1s-2s-3s-4s-1s). From this figure, the values of the water uptake difference (W3-W1) for HKUST-1 material is 0.17 kg_w/kg_{ads} and that of silica gel RD-2060 (W3s-W1s) is 0.088 kg_w/kg_{ads} which yield 93.2% enhancement in the water uptake difference. Similarly, Fig. 14 shows that the water uptake difference for the MIL-100 (0.059) is lower than that of silica gel RD-2060 (0.088) by up to 33%.

Table 4
Adsorption characteristics parameters.

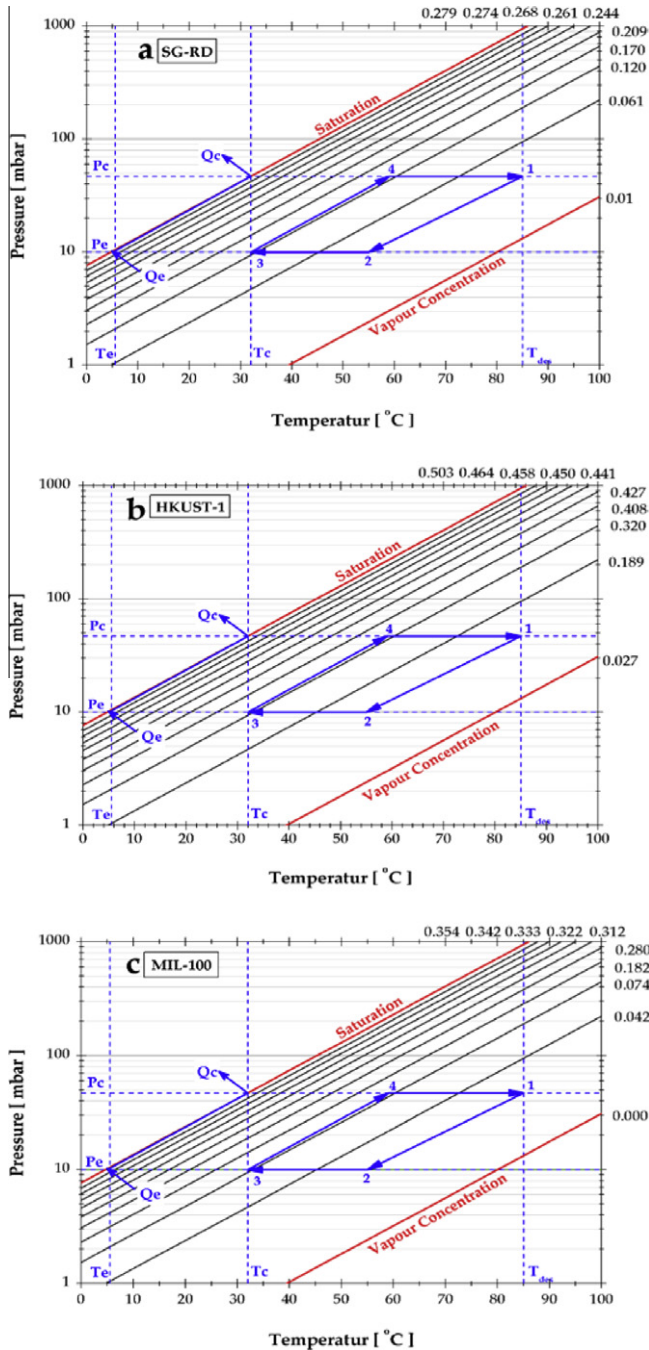| Parameter	Value
A_0	-6.5314
A_1	0.72452×10^{-1}
A_2	0.25493×10^{-6}
A_3	0.25493×10^{-6}
B_1	0.15915
B_2	-0.50612×10^{-3}
B_3	0.53290×10^{-6}

Fig. 13. PTW diagram for different adsorption pair with ideal cycle superimposed.
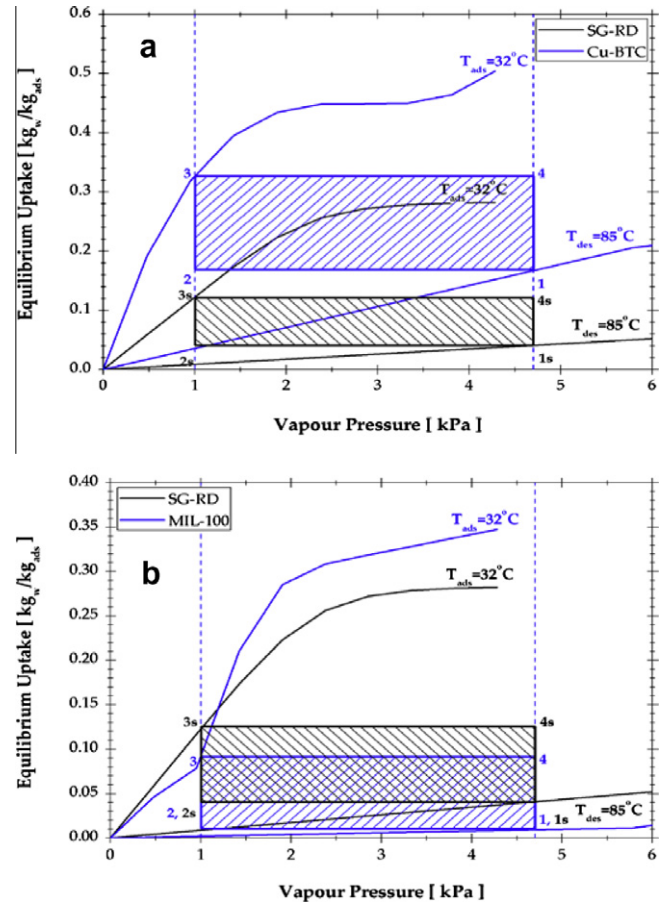

Fig. 14. Comparison of the ideal cycles superimposed on adsorption isotherms.

7. Conclusions

Metal Organic Framework materials have recently attracted extensive research interest for a number of applications like gaseous fuel storage, gas separation and carbon dioxide capture. Regarding water adsorption for cooling application, limited published work is reported. The adsorption characteristics (adsorption isotherms, adsorption kinetics and cyclic performance) of HKUST-1 and MIL-100 MOFs were experimentally investigated and compared to silica gel RD-2060. Results show that HKUST-1/water pair presents the best adsorption characteristics with 93.2% increase in the water vapour uptake difference compared to silica gel RD-2060 at evaporating temperature of 5 °C. This favourable trend is persistent throughout the temperature range tested. HKUST-1 has shown higher capability in adsorbing water vapour than silica gel RD-2060 at low partial pressures. Also, it shows higher adsorption kinetic rates implying shorter adsorption/desorption cycle than that of silica gel RD-2060. However, HKUST-1 has shown significant hysteresis between the adsorption and desorption values indicating thermal instability and need to be further investigated. Results for the MIL-100 have shown an inferior performance compared to that of the silica gel RD-2060 with 33% reduction in the water vapour uptake difference in the cycle at 5 °C. It is important here to point out that this trend for MIL-100 is reversed for evaporating temperatures above 12 °C at the same adsorption, condensation and desorption temperatures. The significance of this finding implies that the MIL-100 can be used in cascade cooling

applications where the evaporation temperature can be higher than 12 °C. The outcome of this work highlights the potential of using MOF materials in water adsorption for cooling applications.

Acknowledgement

References

[1] Z.Z. Xia, C.J. Chen, J.K. Kiplagat, Adsorption equilibrium of water on silica gel, J. Chem. Eng. Data 53 (2008) 2462–2465.
[2] L.X. Gong, R.Z. Wang, Z.Z. Xia, Adsorption equilibrium of water on a composite adsorbent employing lithium chloride in silica gel, J. Chem. Eng. Data 55 (2010) 2920–2923.
[3] Chen, C.J., Wang, R.Z.,Z. Xia, Z., Study on a silica gel-water adsorption chiller integrated with a closed wet cooling tower, Int. J. Thermal Sci. 49 611–620.
[4] S. Li, J.Y. Wu, Theoretical research of a silica gel-water adsorption chiller in a micro combined cooling, heating and power (CCHP) system, Appl. Energy 86 (2009) 958–967.
[5] R.J.H. Grisel, S.F. Smeding, R.D. Boer, Waste heat driven silica gel/water adsorption cooling in trigeneration, Appl. Therm. Eng. 30 (2010) 1039–1046.
[6] R.D. Boer, S. Smeding, S. Mola, Silica gel-water adsorption cooling prototype system for mobile air conditioning. Heat powered cycles, 2009. Technische Universtat, Berlin.
[7] U. Jakob, W. Mittelbach, Development and investigation of a compact silica gel/ water adsorption chiller integrated in solar cooling systems, in: VII Minsk International, seminar, 2008.
[8] W.S. Chang, C.C. Wang, C.C. Shieh, Design and performance of a solar-powered heating and cooling system using silica gel/water adsorption chiller, Appl. Therm. Eng. 29 (2009) 2100–2105.
[9] S.K. Henninger, H.A. Habib, C. Janiak, MOFs as adsorbents for low temperature heating and cooling applications, J. Am. Chem. Soc. (2009) 2776–2777.
[10] S.K. Henninger, F.P. Schmidt, H.M. Henning, Water adsorption characteristics of novel materials for heat transformation applications, Appl. Therm. Eng. 30 (2010) 1692–1702.
[11] H.T. Chua, K.C. Ng, A. Malek, Multi-bed regenerative adsorption chiller â€" improving the utilization of waste heat and reducing the chilled water outlet temperature fluctuation, Int. J. Refrig. 24 (2001) 124–136.
[12] zycon. <http://zycon.hubpages.com/hub/Adsorption-vs-Absorption-Chillers-Applications-Use-Overview>. HubPages 2012 [cited].
[13] D. Saha, S. Deng, Ammonia adsorption and its effects on framework stability of MOF-5 and MOF-177, J. Colloid Interface Sci. 348 (2010) 615–620.
[14] D. Saha, S. Deng, Hydrogen adsorption on metal-organic framework MOF-177, Tsinghua Sci. Technol. 15 (2010) 363–376.
[15] S. Deng, Sorbent technology, Encyclopedia of, chemical processing. http://dx.doi.org/10.1081/E-ECHP-120007963 (2006) 2825–2845.
[16] T. Grant Glover, G.W. Peterson, B.J. Schindler, MOF-74 building unit has a direct impact on toxic gas adsorption, Chem. Eng. Sci., (in press).
[17] P. Küsgens, M. Rose, I. Senkovska, Characterization of metal-organic frameworks by water adsorption, Microporous Mesoporous Mater. 120 (2009) 325–330.
[18] S. Qiu, G. Zhu, Molecular engineering for synthesizing novel structures of metal-organic frameworks with multifunctional properties, Coord. Chem. Rev. 253 (2009) 2891–2911.
[19] Q. Min Wang, D. Shen, M. Bülow, Metallo-organic molecular sieve for gas separation and purification, Microporous Mesoporous Mater. 55 (2002) 217–230.
[20] X.L. Wang, H.T. Chua, L.Z. Gao, A thermogravimetric analyzer for condensable gas adsorption under subatospheric conditions, J. Therm. Anal. Calorim. 90 (2007) 935–940.
[21] X. Wang, W. Zimmermann, K.C. Ng, Investigation on the isotherm of silica gel+water systems TG and volumetric methods, J. Therm. Anal. Calorim. 76 (2004) 659–669.
[22] A. Raymond, S. Garimella, Intraparticle mass transfer in adsorption heat pumps: limitations of the linear driving force approximation, J. Heat Transfer 133 (2011) 042001–42013.
[23] I.I. El-Sharkawy, B.B. Saha, S. Koyama, A study on the kinetics of ethanol-activated carbon fiber: theory and experiments, Int. J. Heat Mass Transfer 49 (2006) 3104–3110.
[24] Y.I. Aristov, M.M. Tokarev, A. Freni, Kinetics of water adsorption on silica Fuji Davison RD, Microporous Mesoporous Mater. 96 (2006) 65–71.
[25] Y.I. Aristov, I.S. Glaznev, A. Freni, Kinetics of water sorption on SWS-1L (calcium chloride confined to mesoporous silica gel): influence of grain size and temperature, Chem. Eng. Sci. 61 (2006) 1453–1458.
[26] B.B. Saha, I.I. El-Sharkawy, A. Chakraborty, Study on an activated carbon fiber-ethanol adsorption chiller: Part I – System description and modelling, Int. J. Refrig. 30 (2007) 86–95.
[27] H.T. Chua, K.C. Ng, A. Malek, Modeling the performance of two bed, silica gel-water adsorption chiller, Int. J. Refrig. 22 (1999) 194–204.
[28] B.B. Saha, S. Koyama, T. Kashiwagi, Waste heat driven dual-mode, multi-stage, multi-bed regenerative adsorption system, Int. J. Refrig. 26 (2003) 749–757.
[29] B.B. Saha, A. Chakraborty, S. Koyama, A new generation cooling device employing CaCl2-in-silica gel-water system, Int. J. Heat Mass Transfer 52 (2009) 516–524.
[30] D.M. Ruthven, Principles of Adsorption and Adsorption Process, First ed., John Wiely & Sons, New York, 1984. pp. 45–70.
[31] I.I. Elsharkawy, B.B. saha, S. Koyama, Experimental investigation on activated carbon-ethanol pair for solar powered adsorption cooling applications, Int. J. Refrig. 31 (2008) 1407–1413.
[32] C.-I. Lin, L.-H. Wang, Rate equations and isotherms for two adsorption models, J. Chin. Inst. Chem. Eng, 39 (2008) 579–585.
[33] M. Llano-Restrepo, M.n.A. Mosquera, Accurate correlation, thermochemistry, and structural interpretation of equilibrium adsorption isotherms of water vapor in zeolite 3A by means of a generalized statistical thermodynamic adsorption model, Fluid Phase Equilib. 283 (2009) 73–88.
[34] F. Stoeckli, T. Jakubov, Water adsorption in active carbons described by the Dubinin–Astakhov equation, J. Chem. Soc. Faraday Trans. 90 (1994) 783–786.
[35] J.J. Mahle, An adsorption equilibrium model for Type 5 isotherms, Carbon 40 (2002) 2753–2759.
[36] B.B. Saha, E.C. Boelman, T. Kashiwagi, Computer simulation of a silica gel-water adsorption refrigeration cycle – the influence of operating conditions on cooling output and COP, ASHRAE Trans. 101 (1995) 348–357.
[37] B.B. Saha, E.C. Boelman, T. Kashiwagi, Computational analysis of an advanced adsorption-refrigeration cycle, Energy 20 (1995) 983–994.
[38] Y. Hamamoto, K.C.A. Alam, B.B. Saha, Study on adsorption refrigeration cycle utilizing activated carbon fibers. Part 2. Cycle performance evaluation, Int. J. Refrig. 29 (2006) 315–327.
[39] O.M. Akpa, E.I. Unuabonah, Small-sample corrected akaike information criterion: an appropriate statistical tool for ranking of adsorption isotherm models, Desalination 272 (2011) 20–26.
[40] X. Wang, H.T. Chua, Two bed silica gel-water adsorption chillers: an effectual lumped parameter model, Int. J. Refrig. 30 (2007) 1417–1426.
[41] A. Akahira, K.C.A. Alam, Y. Hamamoto, Mass recovery adsorption refrigeration cycle–improving cooling capacity, Int. J. Refrig. 27 (2004) 225–234.
[42] A.S. Uyun, A. Akisawa, T. Miyazaki, Numerical analysis of an advanced three-bed mass recovery adsorption refrigeration cycle, Appl. Therm. Eng. 29 (2009) 2876–2884.